

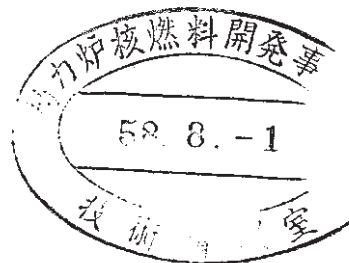
Presented at the 2nd Japanese-German  
Joint Seminar on Nondestructive Evaluation  
and Structural Strength of Nuclear Power  
Plants, 23, 24 February 1983, Tokyo, Japan

# Fracture Toughness of Zr-2.5wt%Nb Pressure Tubes

February 1983

S. Honda, T. Asada  
Power Reactor and Nuclear Fuel  
Development Co.

M. Takeuchi  
Mechanical Engineering Research  
Laboratory, Hitachi Ltd.



Power Reactor and Nuclear Fuel  
Development Corporation

# Fracture Toughness of Zr-2.5wt% Nb Pressure Tubes

by Shun-ichi Honda\*, Takashi Asada\*,  
Mamoru Takeuchi\*\*

## Summary

Measurements of fracture toughness of HT Zr-2.5wt% Nb pressure tubes have been made by studying internally pressurizing (burst) test specimens and small bending test specimens. These tests were conducted from a viewpoint of the effects of hydrogen content, hydride orientation, temperature and crack configuration on the fracture toughness  $K_c$ . Results of the experiments showed that  $K_c$  decreased with increasing hydrogen content, but it would be little affected by hydrogen content at reactor operating temperature. The value of  $K_c$  could be quantitatively evaluated by RHC defined by radial hydride content (RHC) perpendicular to the tensile stress, and it decreased with increasing RHC.

## Nomenclature

$a$  : Crack depth

$c$  : Half crack length

$F$  : Boundary correction factor

$F_N$  : Newman's boundary correction factor

$f_N$  : Modification factor to Newman's

$f_a, f_c, f_r$  : Form factor

$H$  : Width of the bending specimen

$K$  : Stress intensity factor

$K_c$  : Fracture toughness

$K_m$  : Fracture toughness of Zr-Nb alloy that contained no more than 5 ppm hydrogen

$K_{th}$  : Fracture toughness of zirconium hydride

$M$  : Bending moment

$n$  : Constant value for this kind of zirconium alloy

$r$  : Inside radius of the tube

$t$  : Wall thickness

$\theta$  : Angle of inclination of the bending specimen; see Fig.3

---

\*Tokyo Head Office, ATR Section, Power Reactor and Nuclear Fuel Development, 1-9-13, Akasaka, Minato-ku, Tokyo, Japan.

\*\*Mechanical Engineering Research Laboratory, Hitachi Ltd., 3-1-1, Saiwai-cho, Hitachi, Ibaragi, Japan.

$\sigma_g$ : Gross stress

$\sigma_c$ : Fracture stress

## 1. Introduction

Heat treated Zr-2.5wt%Nb alloy is used for pressure tubes of the heavy water moderated, boiling light water cooled reactor, Fugen-HWR, under the operating conditions at about 280°C and 6.8MPa of the coolant. This zirconium alloy pressure tube is embrittled by the presence of hydrogen under certain circumstances. Therefore it is important to assess the embrittlement effect of hydrogen content in order to prevent the unstable fracture of zirconium alloy pressure tubes.

The hydrogen embrittlement of zirconium pressure tubes have been studied, and the effects of hydrogen content, hydride orientation and crack tip configurations were observed [1][2][3]. Watkins et al. [2] studied the effect of hydride embrittlement on critical crack length and showed oriented zirconium hydride could cause embrittlement, wherein the effect of hydrides on critical crack length was observed at lower temperature.

In this paper we present the result of fracture toughness experiments on HT Zr-2.5wt%Nb pressure tube based on burst and bend tests. The experiments were conducted to examine the effects of hydrogen content, hydride orientation, temperature and crack configuration on the fracture toughness. Stress intensity factor equation of a tube with a surface crack is also discussed.

## 2. Pressure Tubes of Fugen-HWR and Test Material

Heat treated Zr-2.5wt%Nb alloy is used for Fugen-HWR pressure tubes because of its good neutron economy and high strength. The pressure tube is 117.8 mm in inside diameter, 4.3 mm in nominal wall thickness and 5,000 mm in length, and is joined to SUS403 Mod. end-fitting by rolled jointing as shown in Fig. 1. It is used under operating conditions of about 280°C and 6.8MPa of light water coolant.

The material investigated is aged, extruded tube made from Zr-2.5 wt%Nb alloy satisfying the specifications for the pressure tubes of the reactor. The heat treatment consisted of water quenching from 870°C, cold drawing to a reduction of 10 ~ 15% and then giving an aging treatment that consisted of holding at 500°C in a vacuum for 24 hours. Its dimensions are 117.8 mm in inside diameter and 4.3 mm in wall thickness.

Four specimens were prepared, each having a different hydrogen content, i.e., 5 ~ 25 (as received), 50, 100 and 250 ppm. The hydrogen was charged by the following method: An 800 mm long tube was shot-blasted on the surface and heated at 450 ~ 500°C in hydrogen gas for a few hours.

Table 1 shows the circumferential mechanical properties of the material.

### 3. Experimental Procedure for Fracture Toughness of Pressure Tubes

#### 3.1 Tube Pressurizing Test (Burst Test)

The full size tube pressurizing test sections were 500 mm long sections of the pressure tube sealed at each end by end caps as shown in *Fig. 1*. A through or half-through wall axial slit was cut at the mid-point of each test section. The slits were cut under oil using an electric discharge machine (EDM) and were typically 0.3 mm wide. The through slit was sealed with 0.1 mm thick stainless steel foil and 2 mm thick rubber sheet stuck on with plastic paste. Hydraulic pressure (silicone oil) was maintained in the test section through one end cap.

The precracked specimens were subjected to the static burst test after fatigue crack occurred. The static burst test at high temperature was performed on the specimen with the heater inside and wrapped outside with thermal insulation.

Small size burst test specimens were also employed for surveillance tests of Fugen pressure tubes. Burst test specimens for surveillance test were 41 mm in inside diameter, 4.3 mm in nominal wall thickness with half-through wall EDM notches. One of the small size burst test specimens had the same dimensions as surveillance test specimens. Dimensions of the other specimen were 57 mm in inside diameter, and 4.3 mm wall thickness. Stress intensity factor equation for a tube with a surface crack will be discussed using these three kinds of tube specimens.

#### 3.2 Bending Test

The special bending test, as shown in *Fig. 3*, was developed to determine fracture toughness. The crescent-shaped specimen cut from the tube is 75 mm in circumference, 30 mm wide and 4.3 mm thick. A sharp notch was cut at the middle on the transverse cross section. As shown in *Fig. 3*, the specimen is set with each end on the jig and inclined by 14.5° from the load axis to avoid out of plane bending at the notch area. A pulsating bending load was applied to the specimen to make a fatigue crack at the root of the notch by three point bending. Afterward, the static bending force was increased until the specimen fracture. This was conducted at several different temperatures.

Specimens were usually loaded after enriching with hydrogen. In some of the specimens, hydrogen enrichment was carried out under bend loading to examine the effect of hydride orientation and of crack tip configuration on fracture toughness. Hydride would be precipitated perpendicular to the tensile stress at crack tips. The tests were carried out under temperature conditions of room temperature to 300°C and hydrogen content of 5 ppm to 300 ppm.

## 4. Results and Discussions

### 4.1 K-equation of Part-Through-Wall Flaw Cylindrical Geometry

Newman's stress intensity factor ( $K$ ) of part-through-wall flaw cylindrical geometry was investigated by using the test results of full size and small size tubular specimens.

*Fig. 4* shows the results of the burst test of 41 mm ID and 57 mm ID, 4.3 mm wall thickness tubes which had EDM notches of 3.3 mm depth on the exterior of the tube. The test was conducted at room temperature and hydrogen content was 10 ppm. The experimental fracture stress values versus crack length are shown together with the values obtained by calculations. Dotted lines show the values calculated by Newman's equation [4], and solid lines show the values calculated by the following equation.

$$K = F\sigma_g \sqrt{\pi c} \quad (1)$$

$$F = f_N F_N \quad (2)$$

$F_N$ : Newman's boundary correction factor [4]

$f_N$ : Modification factor to Newman's; eq. (3)

$$f_N = (f_c)^{f_r} \quad (3)$$

$$f_r = 20(t/r)^2 \quad (4)$$

$$f_c = 2/(1 + (c/a)^{f_a}) \quad (5)$$

$$f_a = 1/(1 + (t/a)^2) \quad (6)$$

Stress intensity factor equation, shown above, was obtained by modifying Newman's equation in order to be able to apply it to small size tubes. Solid lines indicating  $62\text{MPa}\sqrt{\text{m}}$   $K_c$  values calculated by equation (1) in *Fig. 4* show good agreement with experimental results.

*Fig. 5* shows the results for 100 ppm  $H_2$  tube specimens, 41 mm inner diameter, at 150°C. This is a comparison of experimental results and calculational results when the crack depths were varied. Experimental results are almost identical with the line for  $62\text{MPa}\sqrt{\text{m}}$  calculated by equation (1).

The effect of tube diameter on fracture stress was shown in *Fig. 6*. Tube specimens of three diameter sizes, 117 mm ID, 57 mm ID and 41 mm ID, with crack length 20 mm were tested at room temperature, then the hydrogen content of specimens was raised to 250 ppm. Calculations showed values of  $K_c = 22\text{MPa}\sqrt{\text{m}}$  calculated by equation (1). The agreement between calculations and experiments was good.

As shown in *Fig. 4 ~ 6*, it can be concluded that calculations by equation (1) agree well with test results which covered the range of tube diameters from 41 mm to 118 mm, crack depths from 1 mm to 4 mm and crack lengths from 5 mm to 100 mm.

#### 4-2 Comparison of Bend and Burst Test Results and Fracture Toughness of Pressure Tubes

The comparison of burst and bend test results is shown in *Fig. 7 ~ 9*. The relationship between fracture toughness and hydrogen content at room temperature is shown in *Fig. 7*. Stress intensity factor,  $K$  of burst specimens was calculated by equation (1), and the  $K$  of bending specimens was calculated by the following equation [1].

$$K = \sigma_g \sqrt{C} [1.93 - 3.07 \left(\frac{C}{H}\right) + 14.53 \left(\frac{C}{H}\right)^2 - 25.11 \left(\frac{C}{H}\right)^3 + 25.80 \left(\frac{C}{H}\right)^4] \quad (7)$$

$$\sigma_g = \frac{6M}{tH^2 \cos\theta} \quad (8)$$

Although burst test data were widely scattered, their average values were nearly equal to the ones obtained with bend test. These results also show that fracture toughness,  $K_C$  decreased with increased hydrogen content. *Fig. 8* and *Fig. 9* show the effect of test temperature on fracture toughness of 100 ppm and 300 ppm hydrogen content specimens. In *Fig. 8*, fracture toughness values at below 200°C for tubular specimens with half-through EDM notches are higher than values for tubular specimens with through fatigue cracks and bending specimens with fatigue cracks, but the difference between them was not significant. Fracture toughness values were nearly constant at the level of  $50\text{MPa}\sqrt{\text{m}}$  from room temperature to 300°C at this hydrogen content. In case of 250 ppm hydrogen, fracture toughness values increased with temperature, as shown in *Fig. 9*.  $K_C$  values of half through EDM notched tubular specimens were higher than the values of the fatigue crack specimens. However,  $K_C$  values of tubular and bending specimens with fatigue cracks agreed well with each other.

*Fig. 10* shows the effect of hydrogen content at reactor operating temperature, 300°C. The effect of hydrogen content on fracture toughness was very little at 300°C, and the  $K_C$  values were about  $60\text{MPa}\sqrt{\text{m}}$ .

As shown in *Figs. 8* and *9*, fracture toughness values were effected by crack tip configurations. This effect was studied by James and Ostrom [3]. They used fatigue cracks and machined notched tubular specimens, and showed that fracture toughness values of fatigue crack specimens were less than the values of notched specimens. In our experiments this crack tip effect was also studied, using bending specimens with machined notches and fatigue cracks. The specimens were hydrogen enriched up to 160 ~ 210 ppm to investigate the effect of precipitated hydrides which probably orientated perpendicular to the tensile stress at crack tips.  $X$  axis showed this applied net stress. In case of hydrogen enrichment under zero stress, the values of fracture toughness of fatigue crack specimens were less than the values of notched specimens by 30 ~ 40%. These results are very close to the results in *Fig. 9*. However, in case of hydrogen enrichment under stress exceeding  $50\text{MPa}$ ,  $K_C$  values of cracked and notched specimens agreed with each other. These results suggested that fracture toughness would be affected by the hydrides at crack tips or notch roots.

This effect of hydrides on fracture toughness is discussed in the next paragraph.

#### 4.3 Effects of Hydride Orientation

The stress orientation of zirconium hydride is important for pressure tubes because, as noted above, it causes the fracture toughness of the pressure tubes to decrease. Investigation was carried out to determine hydride orientation and its effect on fracture toughness.

The method of the hydride orientation treatment is shown in *Fig. 12(a)*. A tubular specimen is subjected to stress during a thermal cycle. The hydrides were reoriented due to hoop stress as shown in *Fig. 12(c)*. The number of the reoriented hydrides depends on the hydrogen content, stress level and the holding temperature.

*Fig. 13* shows the effect of the hydride reorientation on fracture toughness. The fracture toughness decreased due to the hydride reorientation treatment. Concerning the above results, it is useful to define two terms: Hydride continuity and hydride continuity coefficient (HCC) as shown in *Fig. 14*.

It appears that, HCC is not suitable for estimating the quantitative value of the fracture toughness of zirconium alloy. This is because the maximum value of HCC is 1.0, but the fracture toughness tends to decrease with an increase in the hydrogen content as shown in *Fig. 13*.

Therefore, in this paper a new method of measurement is proposed. A band was chosen along the tube radius on the circumferential section and the length of the hydride projection within the band on the tube radius was measured. In the above measurement, radial hydride content (RHC), which is defined as the total length of the hydrides in a vertical direction projected onto the tensile stress direction per unit area as shown in *Fig. 14*.

*Fig. 15* shows the relationship between the fracture toughness and RHC. The fracture toughness can be expressed as a monotonic curve inversely related to RHC. From the above results, RHC and the fracture toughness  $K_c$  is expressed by following equation.

$$K_c = \left[ \frac{RHC}{1000K_m^n} + \frac{1}{K_{th}^n} \right]^{-\frac{1}{n}} \quad (9)$$

*Fig. 16* shows the relationship between RHC and hydrogen content. As seen from *Fig. 16*, only RHC can be obtained from hydrogen content, and the fracture toughness must be obtained from *Fig. 15*.

## 5. Conclusion

- (1) Fracture toughness was affected by hydride around the crack tip and its values,  $K_{IC}$  decreased with increasing RHC (radial hydride content perpendicular to the tensile stress) by which  $K_{IC}$  could be quantitatively evaluated.
- (2) Fracture toughness values decreased with increasing hydrogen content, but it would be little affected at reactor operating temperature, about 300°C.
- (3) Newman's stress intensity factor equation of a tube with surface crack was modified so as to give good agreement with our experimental results of tube burst tests.
- (4) Almost the same fracture toughness values would be obtained both in bend and burst method.

## References

1. S. Kusumoto, A. Nishioka, et al., "Effects of Hydrogen Content, Temperature, and Crack Configuration on Fatigue Crack Propagation and Unstable Fracture Behaviour of Zr-2.5Nb Pressure Tube, 2nd International Conference on SMiRT, September 1973.
2. B. Watkins, A. Cowan, G.W. Parry, and B.W. Pickles, "Embrittlement of Zircaloy-2 Pressure Tubes", ASTM STP 458, (1969).
3. L.A. James and T.R. Ostrom, "Fracture Behavior of Flawed Zircaloy-2 Pressure Tubes, Nuclear Engineering and Design 14 (1970).
4. J.C. Newman, "Fracture Analysis of Surface and Through Cracks in Cylinder Pressure Vessels, NASA Technical Note D-8325," December 1976.
5. L.G. Bell and R.G. Duncan; Hydrogen orientation in Zr-2.5Nb, AECL-5110, June, 1975.

**Table 1 Circumferential Mechanical Properties of Aged Zr–2.5 Nb Tubing**

Temperature (°C)	Hydrogen Content (ppm)	Ultimate Strength (MPa)	0.2% Proof Stress (MPa)	Elongation (%)	Reduction in Area (%)
R. T.	0	859	778	18.8	48.5
	50	781	684	13.7	43.3
	300	721	614	12.1	32.4
300	0	585	—	18.0	64.0
	50	516	—	27.3	64.5
	100	512	—	21.1	63.0
	300	486	—	15.3	59.3

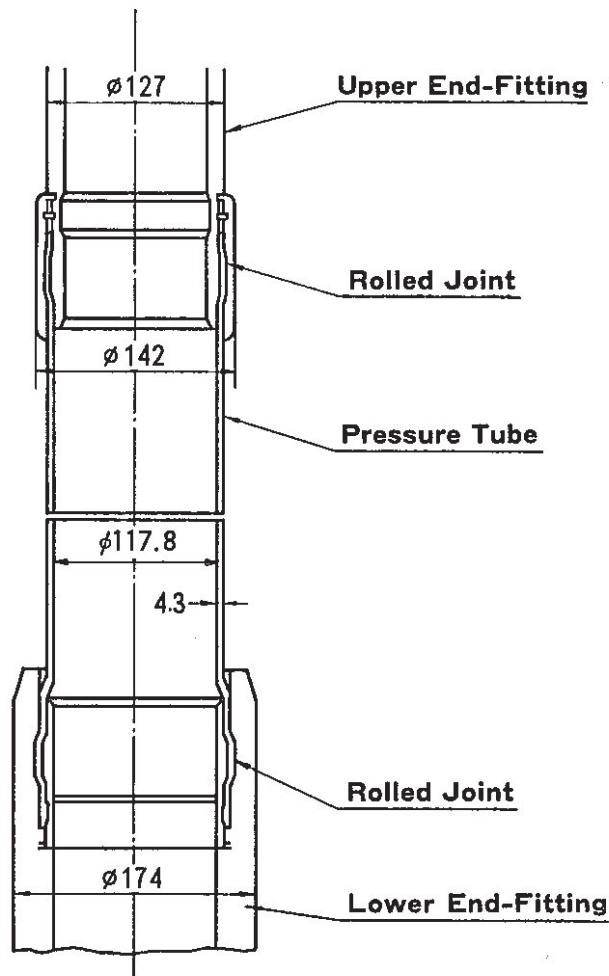


**Fig. 1 Pressure Tube Assembly of Fugen-HWR**

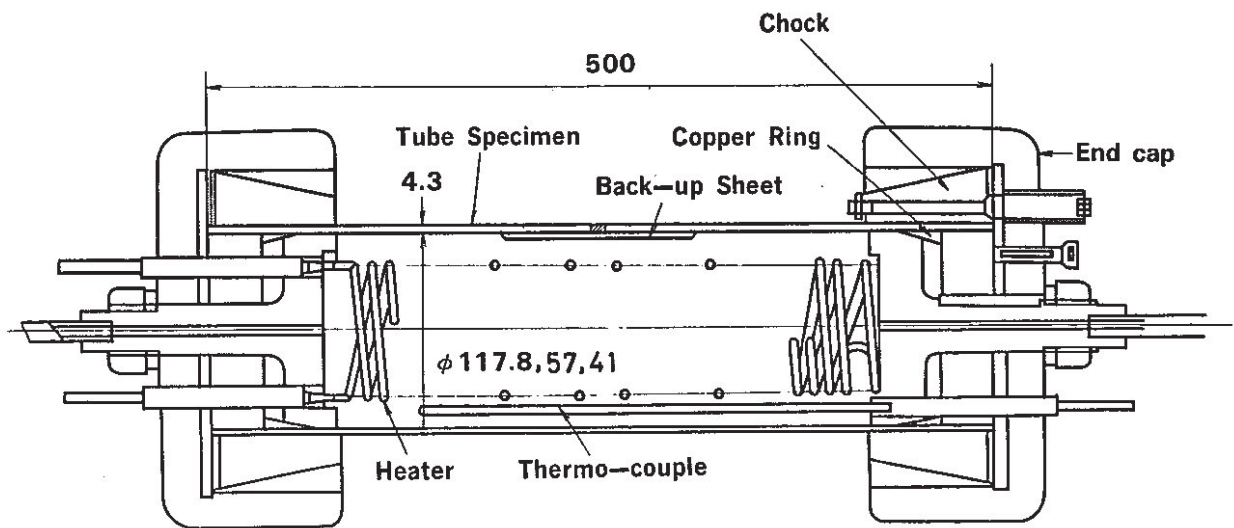
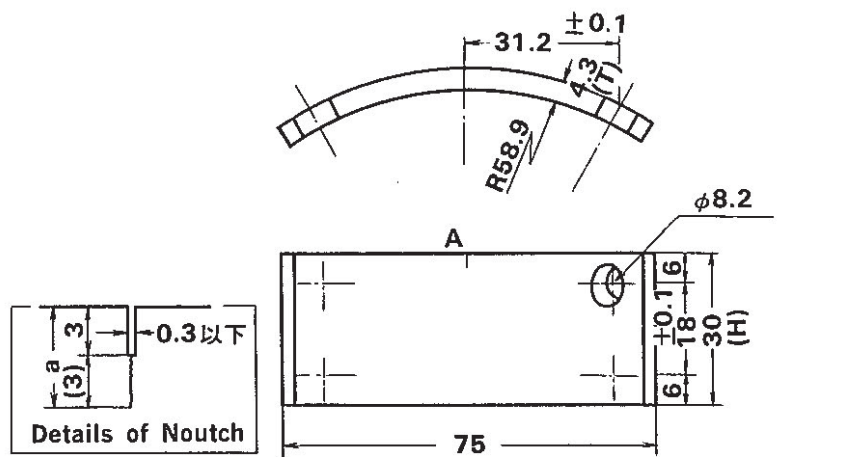
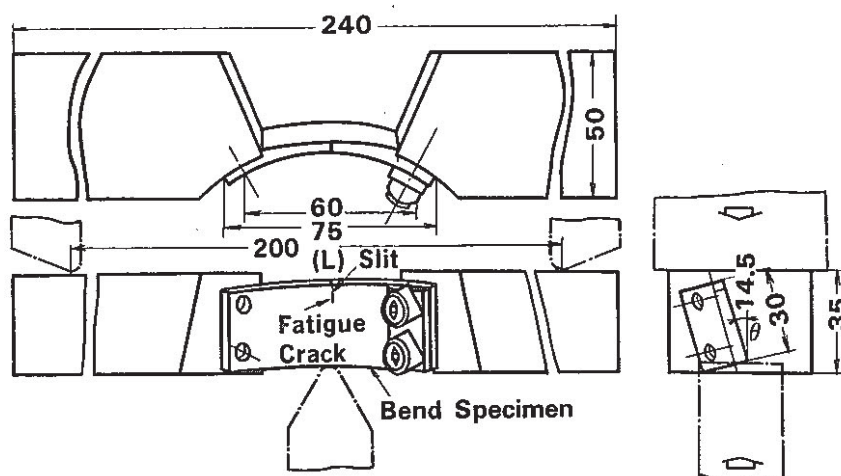


**Fig. 2 Construction of Specimen Assembly for Internal Pressurizing Test.**



**(a) Details of Bend Specimen (Type I)**



**(b) A Specimen and the Loading Fixture for Bend Test**

**Fig. 3 A Specimen and the Loading Fixture for Bend Test. (Type 1 Specimen)**

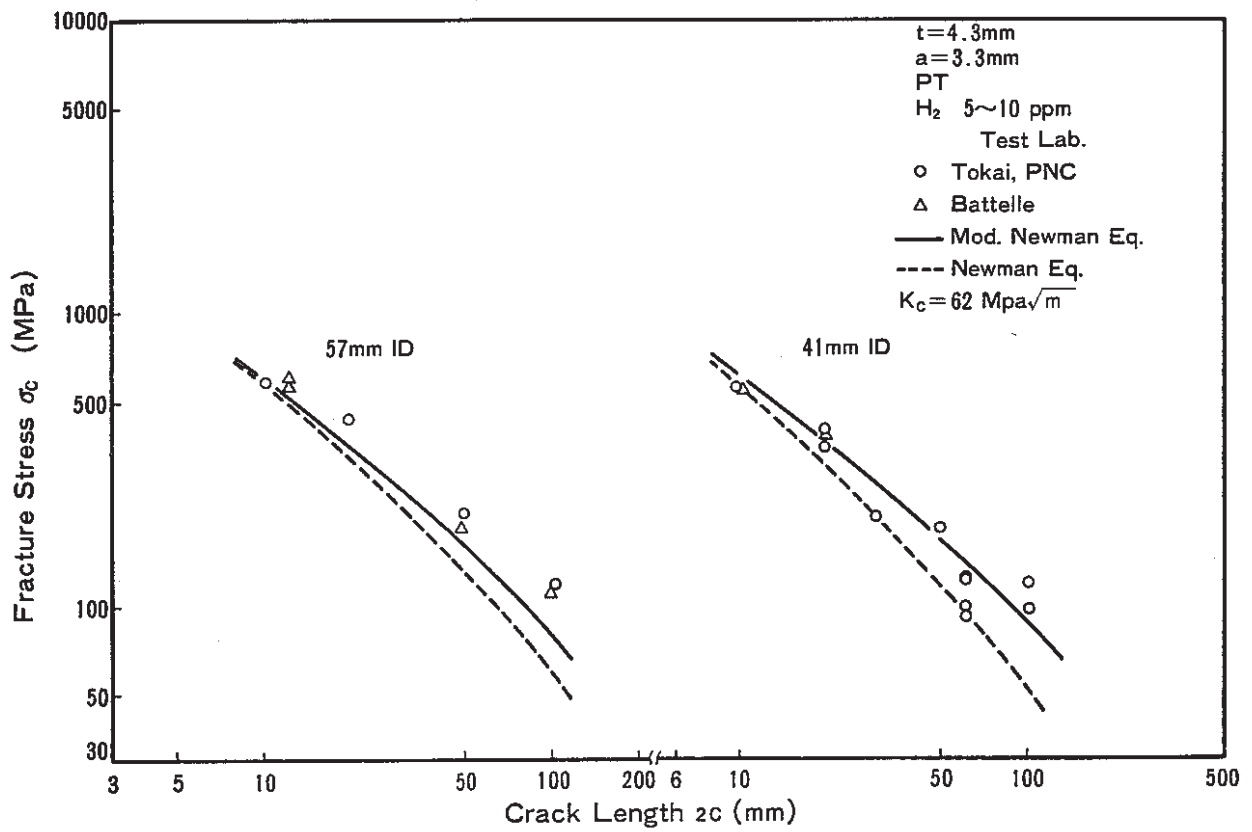


**Fig.4 Comparison of Experimental Results and Calculations by Mod. Newman eq. on Burst Test**

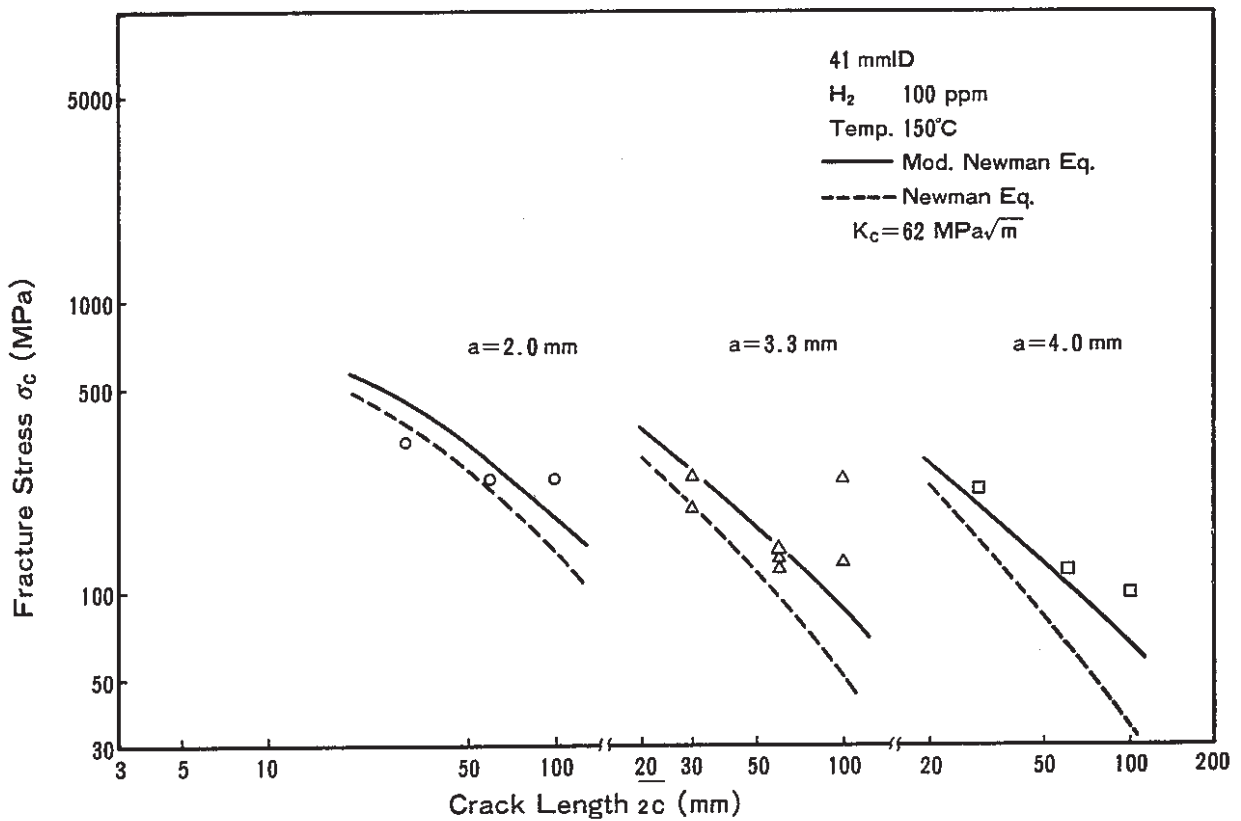


**Fig.5 Comparison of Experimental Results and Calculations by Mod. Newman eq. on Burst Test**

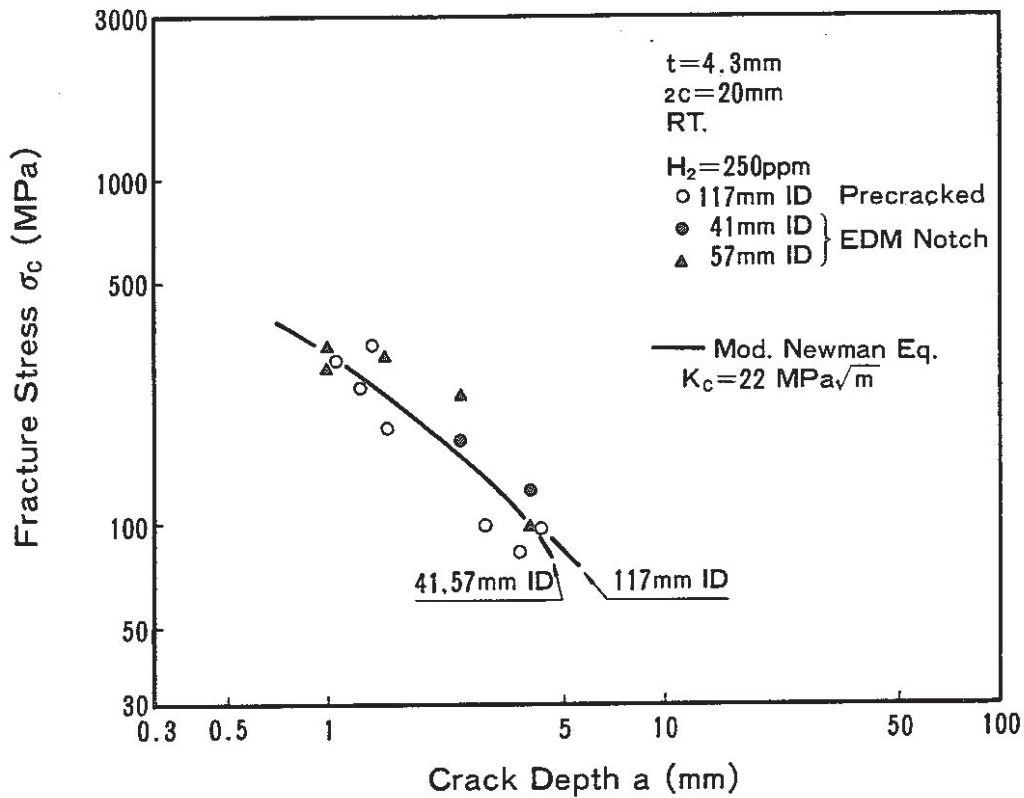


**Fig.6 Effect of Crack depth on Fracture stress, and Comparison of Experimental Results and Calculations by Mod. Newman eq. on Burst Test**

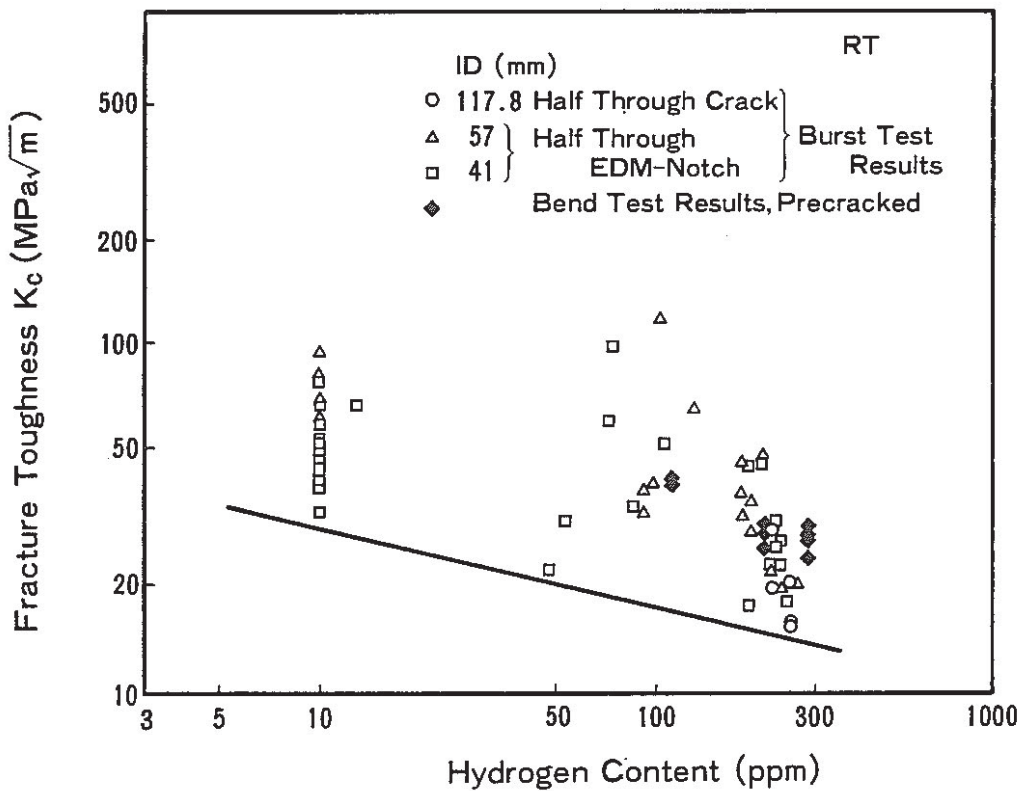


**Fig.7 Comparison of Bend and Burst Test Results at RT**

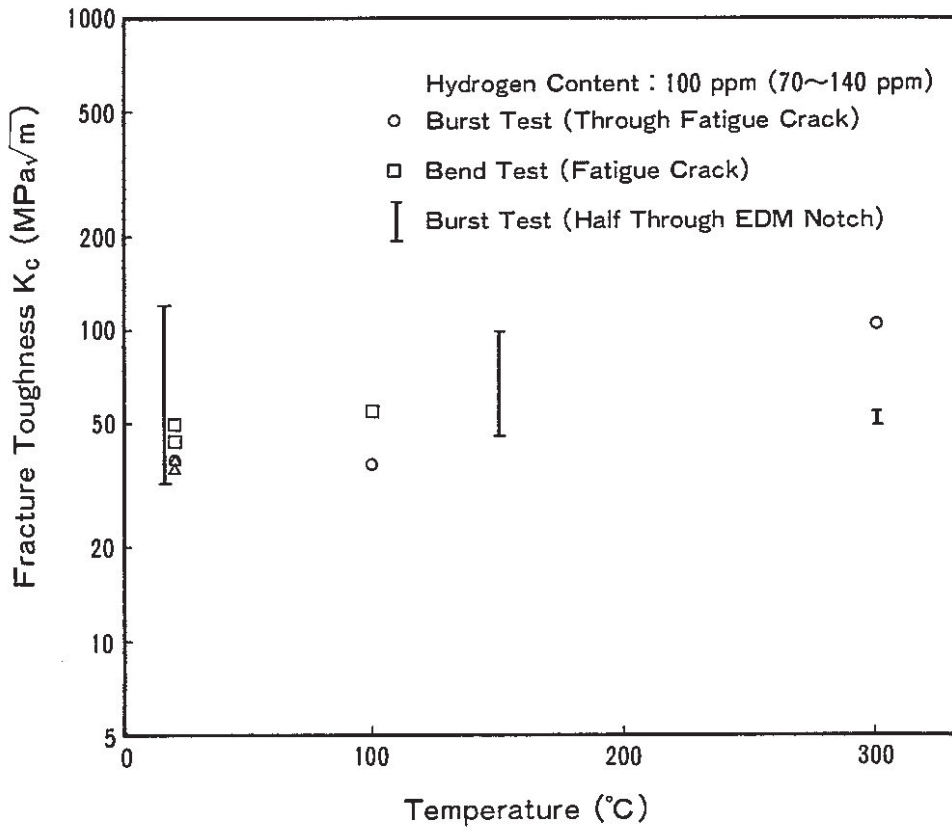


**Fig.8 Fracture Toughness for 100 ppm Hydrogen Enrichment Specimens**

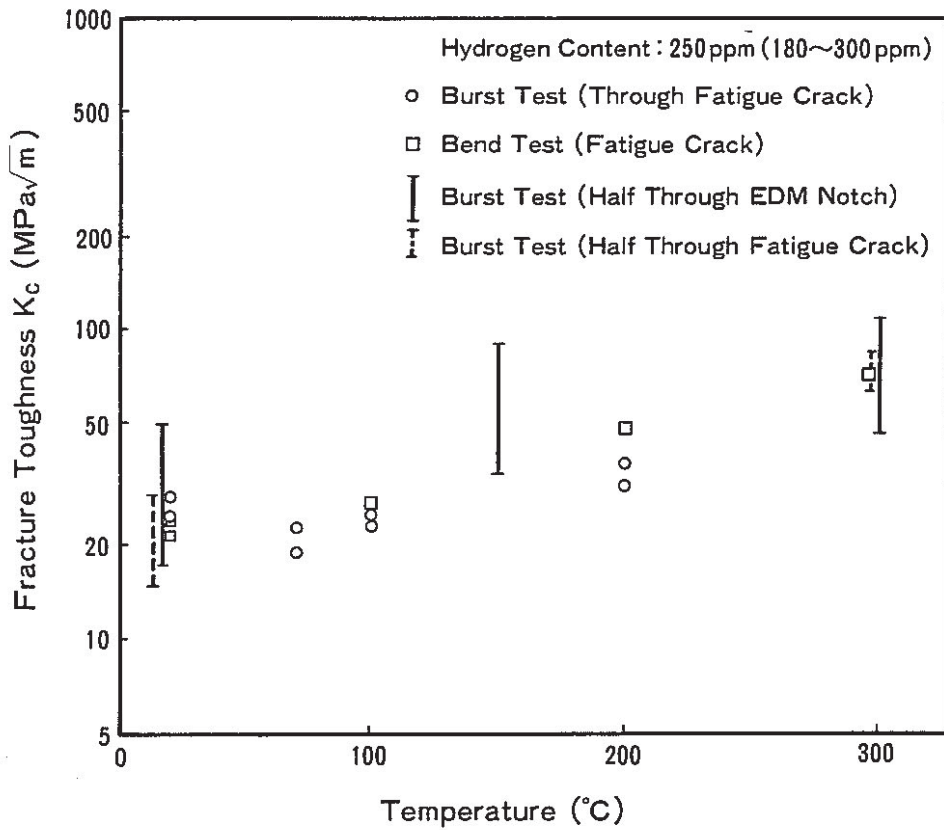


**Fig.9 Fracture Toughness for 300 ppm Hydrogen Enrichment Specimens**

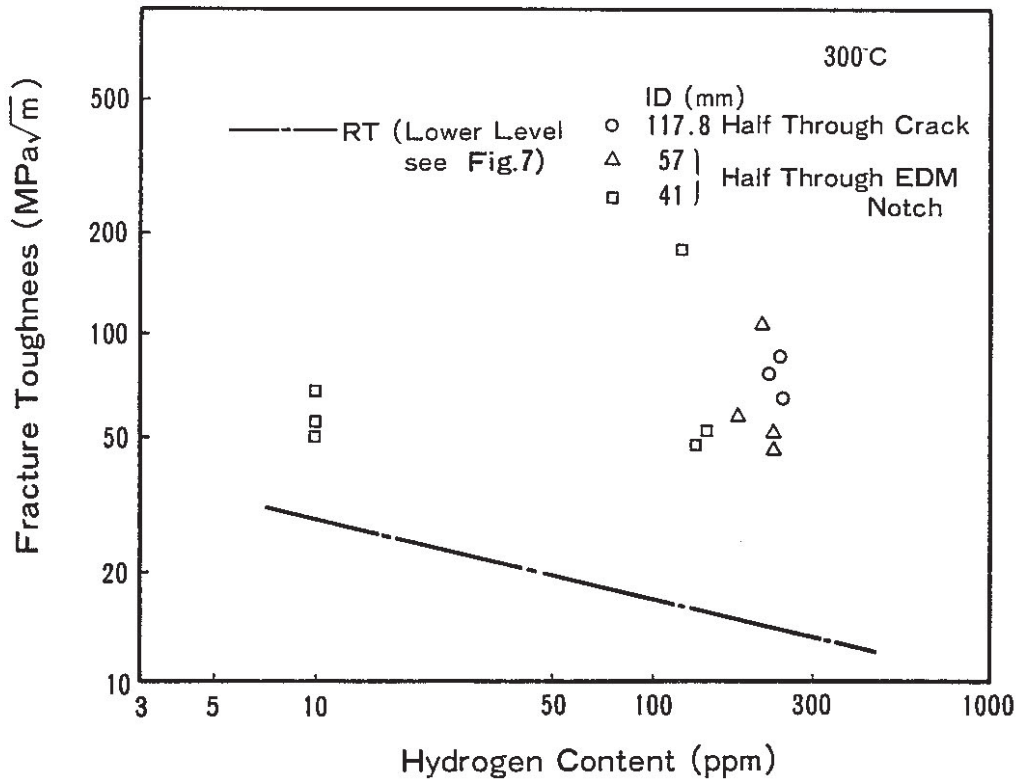


Fig. 10 Fracture Toughness at 300°C

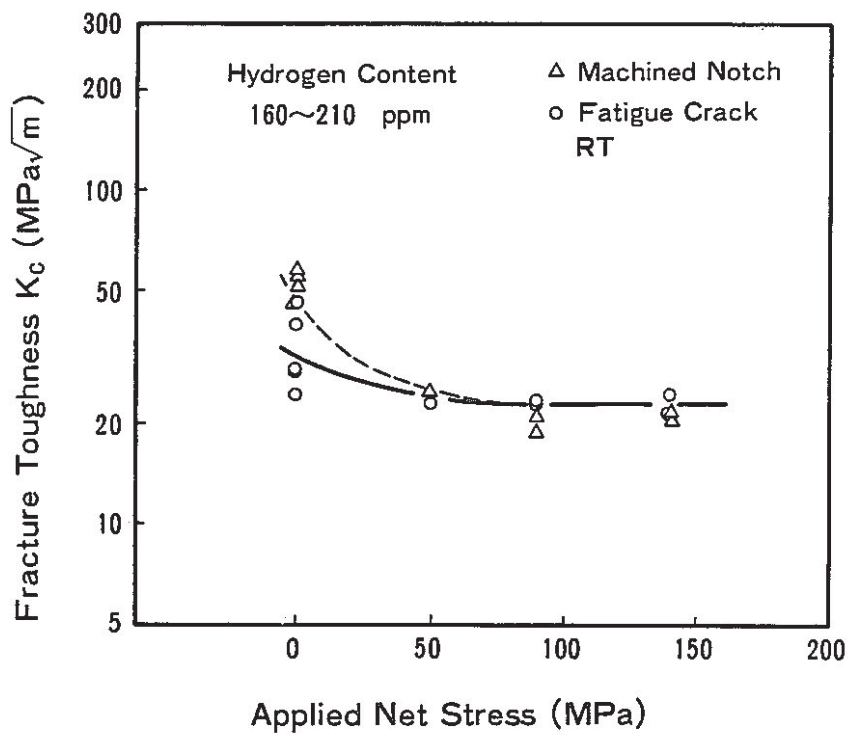


Fig.11 Effect of Applied Stress on Fracture Toughness : Hydrided under Stress

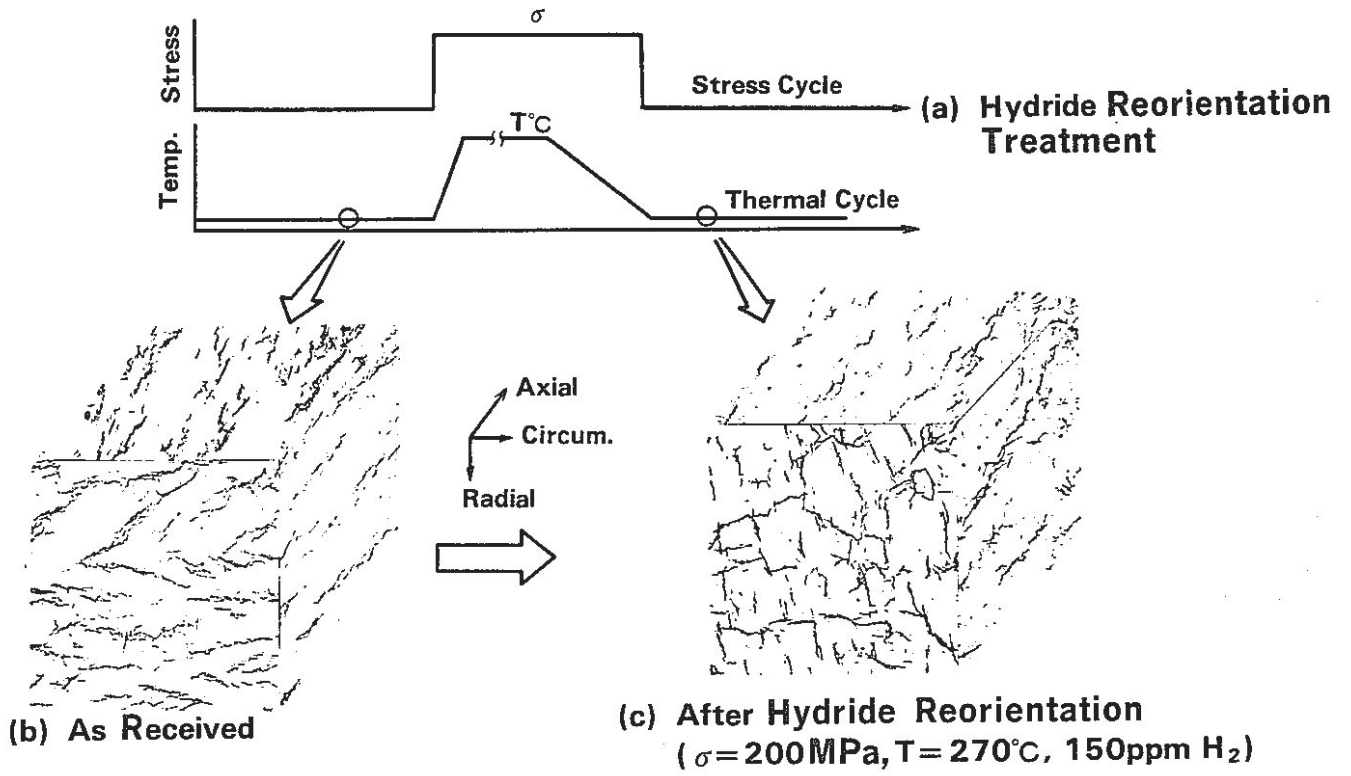


Fig.12 Hydride Reorientation Treatment and Hydride Distribution

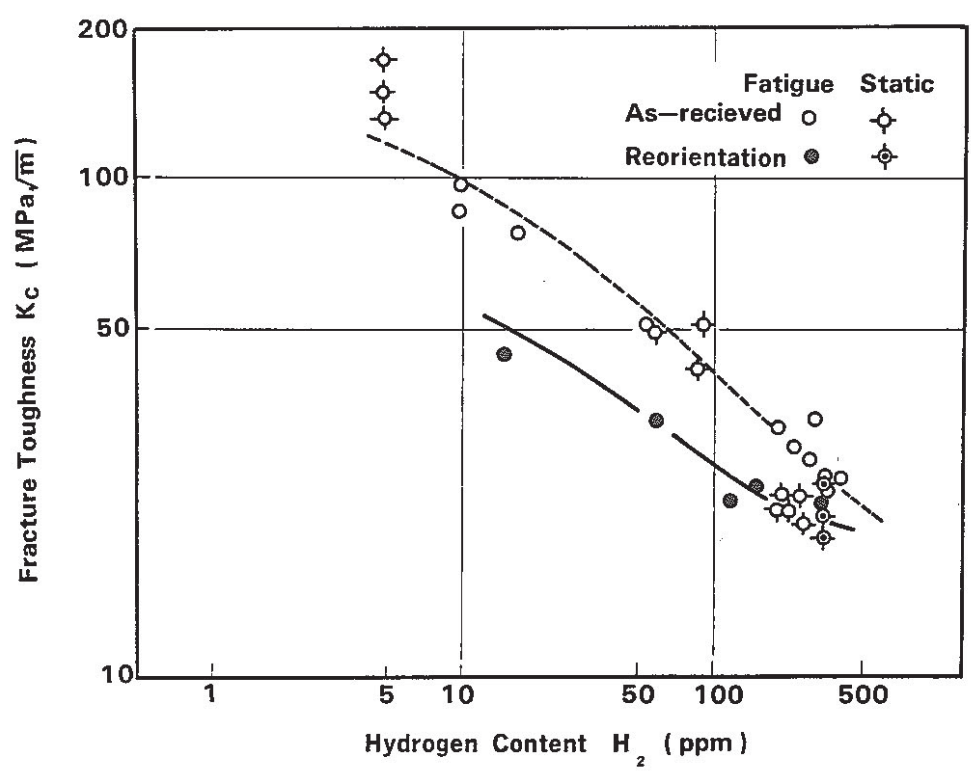
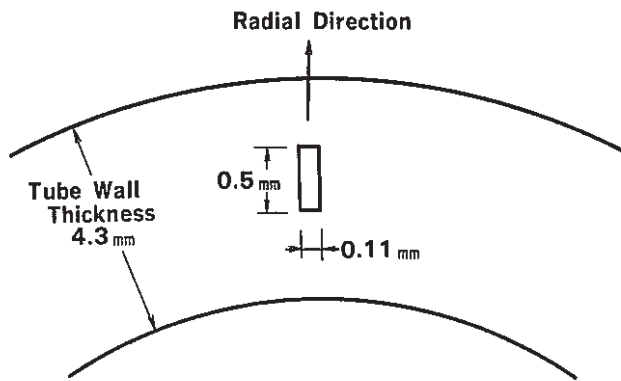


Fig.13 Relationship Between RHC and Hydrogen Content



A Section of Perpendicular to the Pressure Tube Axis Showing size and Position of Hydride Continuity Band

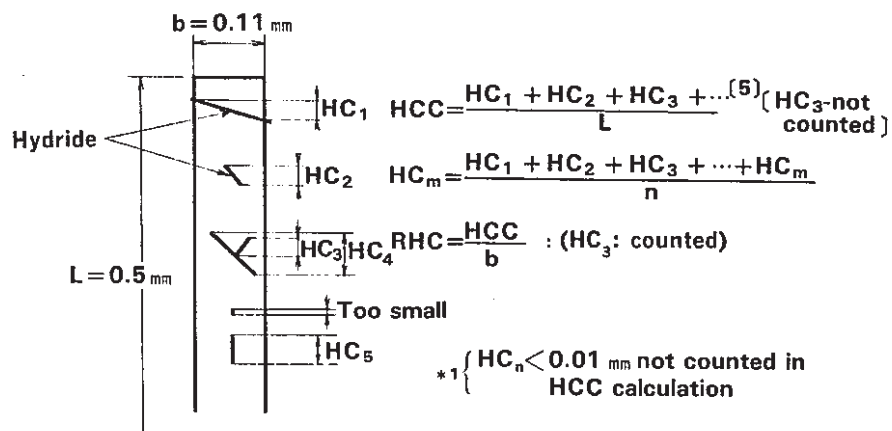


Fig.14 Schematic Illustration of RHC

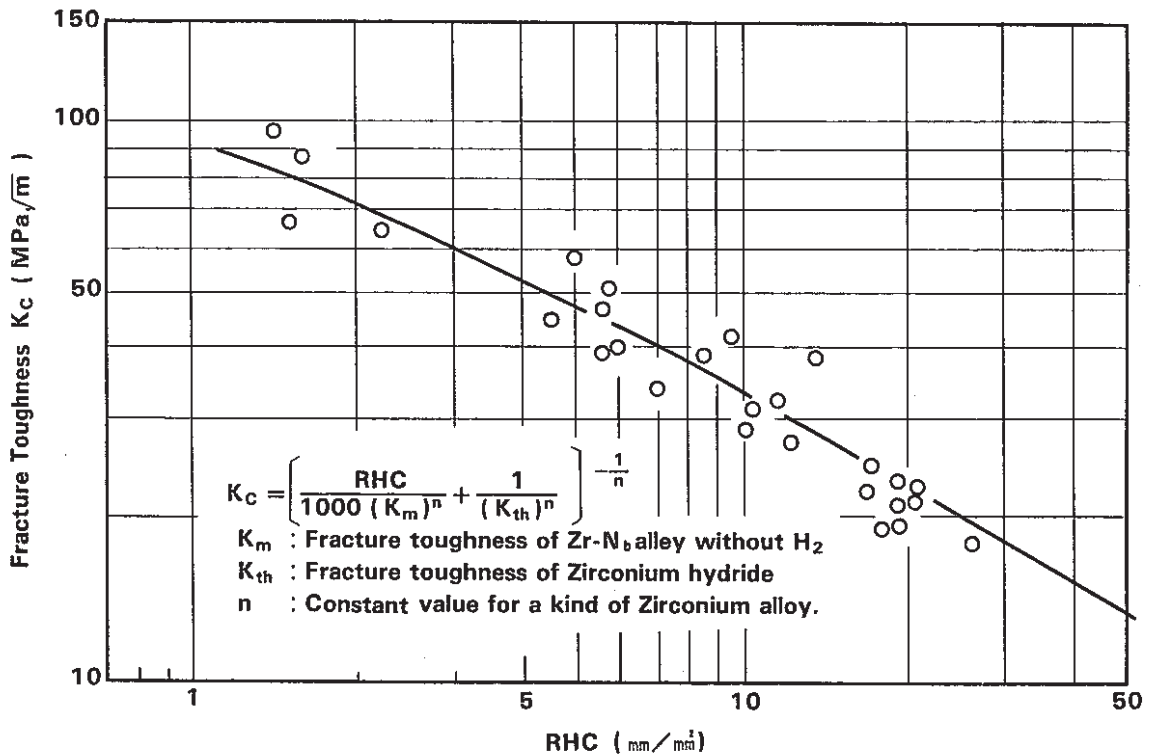
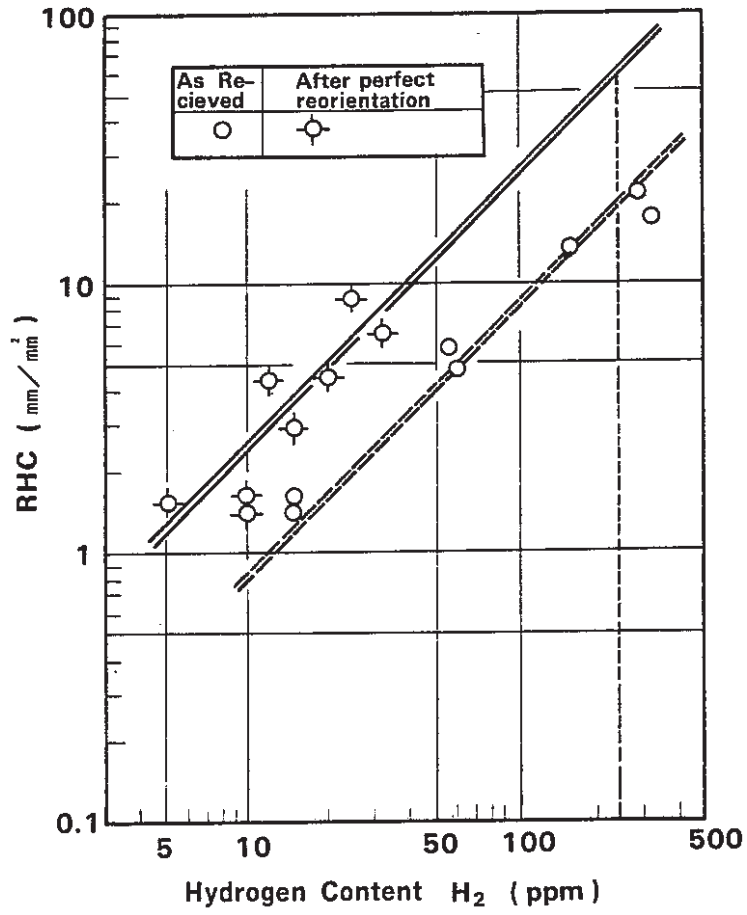


Fig.15 Effect of Hydride Reorientation on the Fracture Toughness



**Fig.16 Relationship Between RHC and Fracture Toughness**